Engineering Research
Express



**PAPER**

# Exploring low-velocity impact performance of zirconium dioxide-infused jute/epoxy composites

To cite this article: Dharshini Devi *et al* 2025 *Eng. Res. Express* **7** 0455c7

IOP Publishing Eng. Res. Express 7 (2025) 0455c7 https://doi.org/10.1088/2631-8695/ae2760

Engineering Research Express

Check for updates

RECEIVED
21 May 2025

REVISED
27 October 2025

ACCEPTED FOR PUBLICATION
1 December 2025

PUBLISHED
16 December 2025

PAPER

# Exploring low-velocity impact performance of zirconium dioxide-infused jute/epoxy composites

**Dharshini Devi**[1], **Chandrasekar Muthukumar**[1,*], **Senbagan Muthusamy**[2], **Senthilkumar Krishnasamy**[3,*] and **Senthil Muthu Kumar Thiagamani**[4,5,6]

[1] SIMCRASH Centre, Department of Aerospace Engineering, Hindustan Institute of Technology & Science, Kelambakkam, Chennai 603103, India
[2] Department of Aeronautical Engineering, Dhanalakshmi Srinivasan College of Engineering and Technology, Mamallapuram, Tamilnadu, India
[3] Department of Mechanical Engineering, PSG Institute of Technology and Applied Research, Coimbatore, Tamil Nadu, India
[4] Department of Mechanical Engineering, Kalasalingam Academy of Research and Education, Anand Nagar, Krishnankoil 626126, Tamil Nadu, India
[5] Mechanical Engineering Department, Faculty of Engineering and Quantity Surveying, INTI International University, Persiaran Perdana BBN, Putra Nilai, 71800 Nilai, Negeri Sembilan, Malaysia
[6] Centre for Advanced Composite Materials (CACM), Universiti Teknologi Malaysia, 81310 Skudai, Johor Bahru, Johor, Malaysia
[*] Authors to whom any correspondence should be addressed.

**E-mail:** chandrasekar.25j@gmail.com and kmsenthilkumar@gmail.com

**Keywords:** natural fibre, jute, drop-weight impact, ultrasonic C-scan, zirconiun dioxide nanoparticles, nanocomposite

## Abstract

This investigation elucidates the drop-weight impact performance of the jute/epoxy composite laminates infused with zirconium dioxide ($ZrO_2$) at a filler loading of 5%, 10% and 15% in terms of weight by means of ultrasonication. The results reveal that the peak load increased almost linearly with filler addition for 5 wt% and 10 wt% $ZrO_2$ composites by 18% and 27% respectively. In contrast, a gradual reduction in energy absorption was observed, with values decreasing by 9% and 15% at 10 wt% and 15 wt% $ZrO_2$ loading. Damage assessment using both digital image analysis and ultrasonic C-scan demonstrated that the surface damage area was reduced by approximately 22% and 35% for 5 wt% and 10 wt% $ZrO_2$ composites, respectively, relative to the baseline, corroborating the improvement in peak load. A relationship between the damage area and peak force as well as absorbed energy were established and it provides a demarcation between the aforementioned parameters with respect to the filler $ZrO_2$ loading.

## 1. Introduction

The increasing interest in natural fiber-reinforced composites for the industrial and high-performance applications are associated with their advantages like biodegradability, low density, and cost-effectiveness [1–3]. Absorbed energy, peak force and damage area are the typical performance metrics evaluated for a composite material subjected to the drop-weight impact performance where the strike velocity of the impactor ranges from 1 m s−1 to 10 m s−1. Key factors influencing the response to LVI of a polymer composite, includes fiber orientation, stacking sequence, laminate thickness, impactor geometry, impact energy, and matrix type [4, 5]. Strategies to enhance impact resistance of the natural fibre reinforced composites are hybridization incorporating other synthetic fibers or other natural fibers, chemical pre-treatment of fibers, adding nano-fillers, and modifying fiber architecture [6, 7]. Optimizing these parameters can improve impact resistance and damage tolerance of such composites. Nanofillers are increasingly used in biocomposites for their ability to enhance the strength and to improve the interfacial adhesion between the fibre and matrix by adding them at small weight fractions [8–10]. The topic of interest to this work is to assess the influence of zirconium dioxide ($ZrO_2$) on the drop-weight impact performance of the jute/epoxy composite. $ZrO_2$ have been selected as nanofiller due to its high fracture toughness and resistance to cracking which are inevitable characteristics for

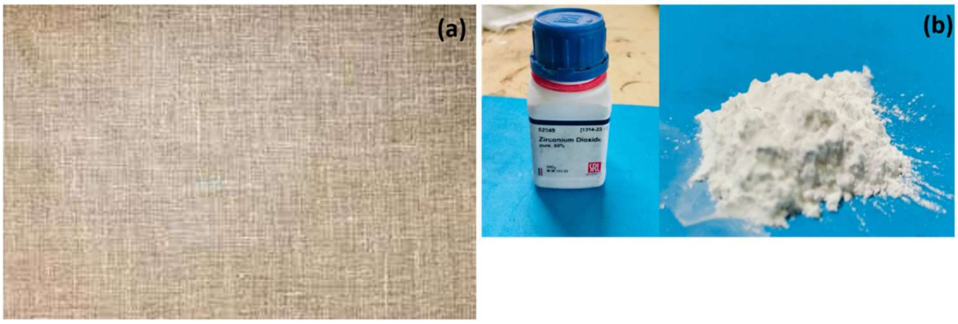


**Figure 1.** Reinforcements (a) Jute Fabric and (b) $ZrO_2$ Nanoparticles.

superior impact resistance of the composite. In addition to it, the other advantages such as low thermal conductivity, biocompatibility, enhancing strength and low wear rates makes them a potential filler for high-perfomance applications [11, 12].

This section summarizes the findings from literature on the $ZrO_2$ dispersed composites. Prasob and Sasikumar demonstrated that incorporating 2 wt% $ZrO_2$ in the jute/epoxy composite enhanced the tensile strength, flexural strength, compressive strength and inter-laminar shear strength and the $ZrO_2$ infused jute/epoxy composite exposed to sub-zero temperature did not affect the load bearing ability and even shown to have better mechanical properties than at room temperature. The improvement in mechanical properties were credited to the better interfacial adhesion promoted by the presence of $ZrO_2$ [13]. In their another work, mechanical properties of jute/epoxy composites infused with $ZrO_2$ and titanium dioxide ($TiO_2$) was examined with 2%, 4%, and 6% in terms of filler weight at room temperature and sub-zero temperatures of −20 °C and −40 °C. Both the fillers were able to improve mechanical properties under tensile, flexural and compression load upto 4 wt% and further increase to 6 wt% filler led to decline in strength [14]. In a recent study, Lohbauer *et al* revealed that incorporating incorporating zirconia nanoparticles from 5 wt% to 20 wt% improves the microtensile bond strength (μMBS) of the primer and adhesive used for dental applications. μMBS tend to increase with the filler addition upto 20 wt%. Their study also revelaed that nanofiller dispersion in the primer and adhesive makes significant difference to the μMBS where dispersing in the primer was found to effectively increase the μMBS than in the adhesive [15].

Jute fibre was selected as the reinforcement owing to the advantages including their low cost, biodegradability, and abundance, while offering a reasonable balance of tensile strength and stiffness, making it a suitable reinforcement for intermediate load-bearing applications. Epoxy resin has better compatibility with natural fibres in terms of adhesion and helps to minimize voids in the composite. $ZrO_2$ was selected among the other fillers because of its matrix toughening effects which helps in resisting crack propagation and thereby, improved energy absorption and damage tolerance under impact loading. The increment in filler content was intended to identify an optimal loading level and provides critical insights into the role of filler content on the impact resistance and structural integrity of the nanocomposite.

The research works carried out on the $ZrO_2$ infused jute/epoxy composites were primarily focused on exploring the static mechanical properties. Moreover, the energy absorption charcteristics and damage area assessment of the jute fibre reinforced composite subjected to drop-weigh impact performance in terms of fibre architecture, laminate thickness, different impactor energies, impactor mass and impactor geometry has been well documented [16]. However, the literature lack studies in understanding how the specific combination of zirconium dioxide and jute/epoxy composites influences the dynamic behavior of composites under impact load in the low velocity impact regime. This article represents a missed opportunity to comprehensively assess the impact resistance of $ZrO_2$ infused jute/epoxy composites and their interaction at different proportions of the filler. The approach integrates C-scan imaging to accurately capture subsurface damage morphology, thereby providing a more reliable assessment of crack propagation and damaged area compared to optical image-based tools.

## 2. Materials and method

### 2.1. Materials

A woven jute fabric (250 GSM) as shown in figure 1 was purchased from the Go Green Products Pvt Ltd, Chennai, India. Araldite LY556 epoxy resin and HY951 Hardener was purchased from Hayael Aerospace,

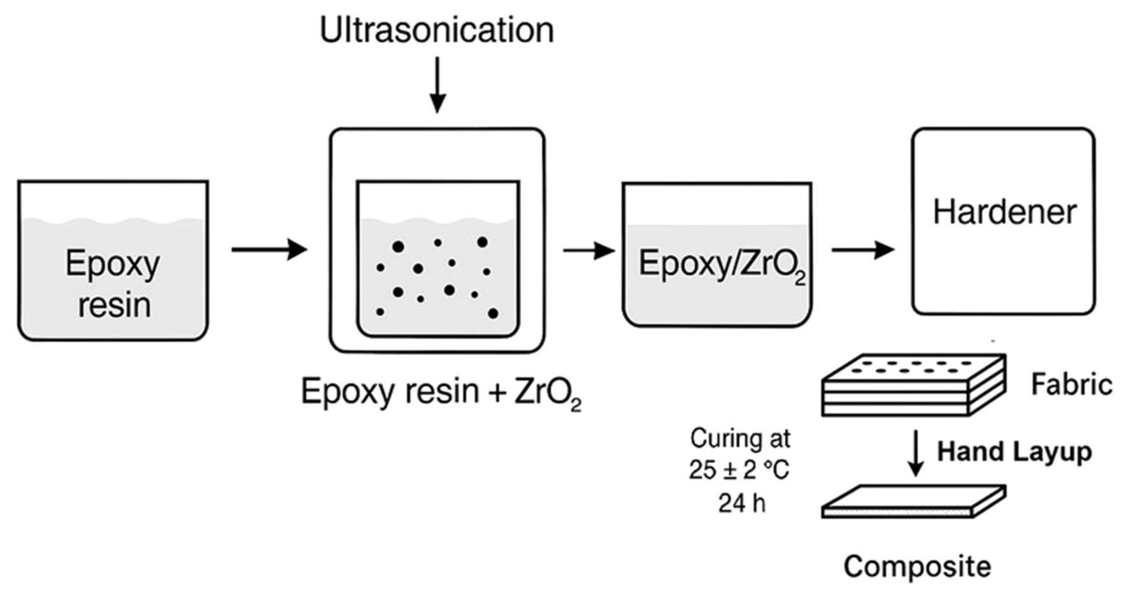


**Figure 2.** Schematic of the fabrication process.

**Table 1.** Specifications of the reinforcement and matrix.

| Properties | Jute [17] | Epoxy |
|---|---|---|
| Density (g/cm$^3$) | 1.3 | 1.15–1.20 |
| Tensile strength (MPa) | 393–773 | 82 |
| Young's Modulus (GPa) | 26.5 | — |
| Elongation % at break | 1.5–1.8 | — |
| Viscosity (mPa.s) | — | 10–12 |

**Table 2.** Major properties of $ZrO_2$ filler.

| Properties | $ZrO_2$ filler |
|---|---|
| Color | White |
| Particle size (nm) | 123.22 |
| Melting point (°C) | 2700 |
| Boiling point (°C) | 5000 |

**Table 3.** Composite configurations.

| Notation | Jute fabric (wt%) | Epoxy & hardener (wt%) | $ZrO_2$ (wt%) |
|---|---|---|---|
| Z0 | 50 | 50 | 0 |
| Z5 | 50 | 45 | 5 |
| Z10 | 50 | 40 | 10 |
| Z15 | 50 | 35 | 15 |

Chennai. Zirconium dioxide ($ZrO_2$) filler was obtained from the Sisco laboratories private limited. Specifications and properties of the reinforcement and matrix are given in tables 1 and 2.

### 2.2. Fabrication method

The fabrication of the composite is done through Hand layup process with jute fabric as reinforcement and epoxy resin as matrix dispersed with zirconium dioxide fillers as shown in figure 2. The reinforcement to matrix was maintained as shown in the table 3.

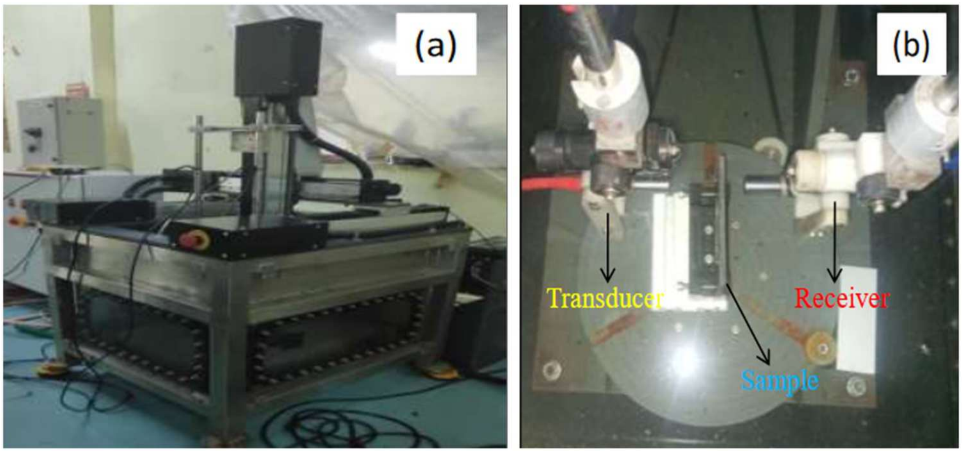


**Figure 3.** Ultrasonic C scan setup (a) 'Through-the-immersion' type and (b) Specimen setup inside the water bath.

Initially, the epoxy resin was taken in a container and mixed with different proportions of $ZrO_2$ nanofiller through ultasonification process. Then, the hardener was mixed with resin in 1:10 ratio as recommended by the resin manufacturer and poured onto the 6 fabric layers of 120 mm × 120 mm (Length × Width) placed on a sheet metal coated with releasing agent. The resin mixture was then gently spread through the fabric layers and the setup was cured at room temperature for 24 h. The fabricated composites had a nominal thickness of 3.5 mm.

### 2.3. Drop weight impact test

Drop weight impact test was performed using the CEAST FRACTOVIS PLUS machine at Madras Institute Technology, Chrompet, Chennai, India as per the ASTM D5628 [18]. The experiment was carried out at an incident energy level of 10 J corresponding to a height of 530 mm and impact velocity of 3.22 m $s^{-1}$. The data acquisition system provides load-time history, energy absorbed and displacement with respect to time. The impactor was a cylindrical rod with hemispherical nose diameter of 20 mm and a total mass of 1.926 kg (includes carrier mass of 1.3 kg and impactor mass of 0.626 kg).

### 2.4. Ultrasonic C-scan

The extent of damage on the impacted specimen was assessed using 'Through-the-immersion' type ultrasonic C-scan which operates in the transmission mode. The C-scan facility located at Dhvani Research & Development Solutions, Perungudi, Chennai, India was utilized (figure 3). A transducer frequency of 5 MHz and a scan resolution of 0.5 mm for both the index and scan axes was employed. This ensured that even minute details could be accurately captured and analyzed. Additionally, the scan length was defined as 100 mm for both the index and scan axes, providing sufficient coverage of the specimen under examination. Following the collection of ultrasonic images, the next step involved the calculation of the damage area and measurement of crack length using the 'SketchAndCalc' platform. This platform provides instant area based on the mapping of damage area and dimension of the sides arund the damage zone.

## 3. Results and discussion

### 3.1. Influence of zirconia addition on the peak force and energy absorption

Figures 4(a)–(d) represents the overall load-time history of the jute/epoxy composite with and without $ZrO_2$ fillers. At the initial stage, the spike in load occurs due to the contact of hemispherical impactor with the composite laminate. The load exhibited a linear increase until $P_{threshold}$ which is the point of initiation of failure in the form of matrix crack. The immediate inflection point after the $P_{threshold}$ represented by $P_{critical}$ is the point where the inititated matrix crack propagates further. $P_{threshold}$ indicates the boundary between elastic and plastic limit while the $P_{critical}$ is the point beyond which the cracks may progress leading to interfacial de-bonding in the composite laminate. The composite specimen continued to endure the impact load further until $P_{max}$ attaining the peak value between 4 ms to 6 ms and the force diminishes significantly indicating final failure of the composite material.

An interesting observation from the load—displacement plot for the composites Z0, Z5 and Z10 is that there was a substantial difference between $P_{critical}$ and $P_{threshold}$ where the former had higher magnitude.

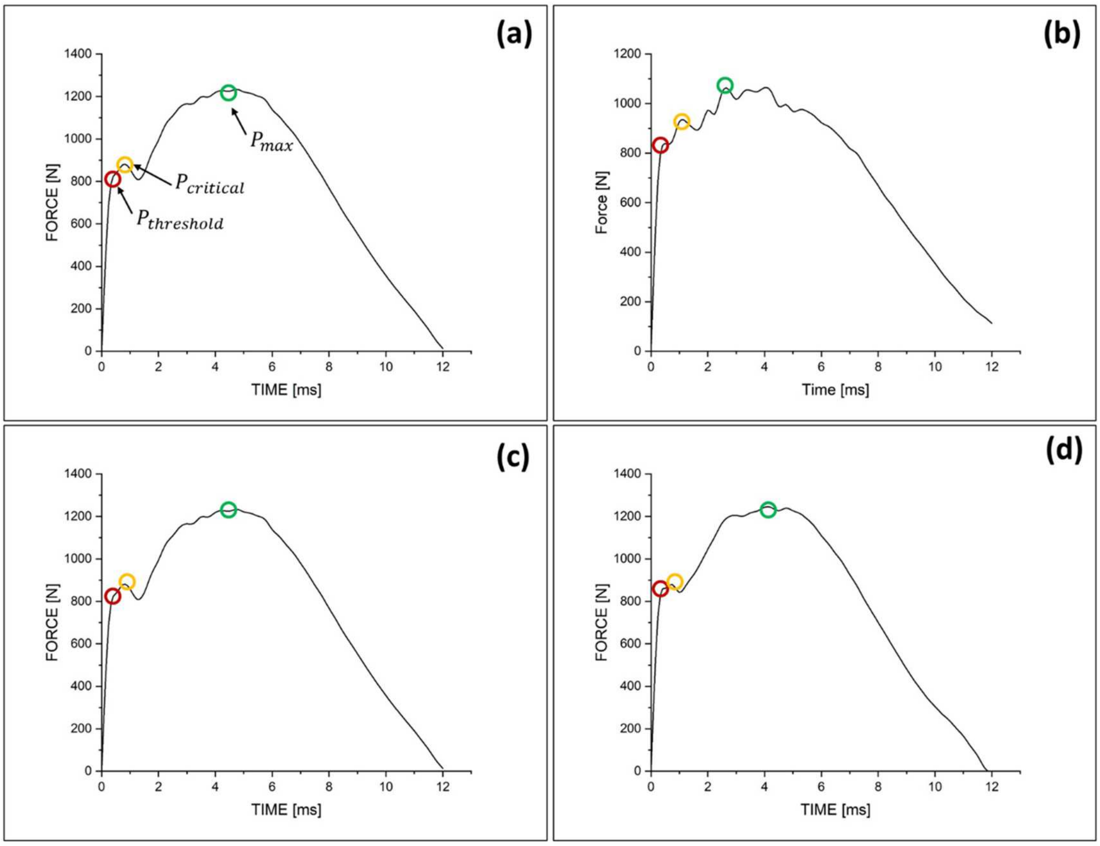


**Figure 4.** Load—time plot from the drop weight impact test (a) Z0, (b) Z5, (c) Z10 and (d) Z15.

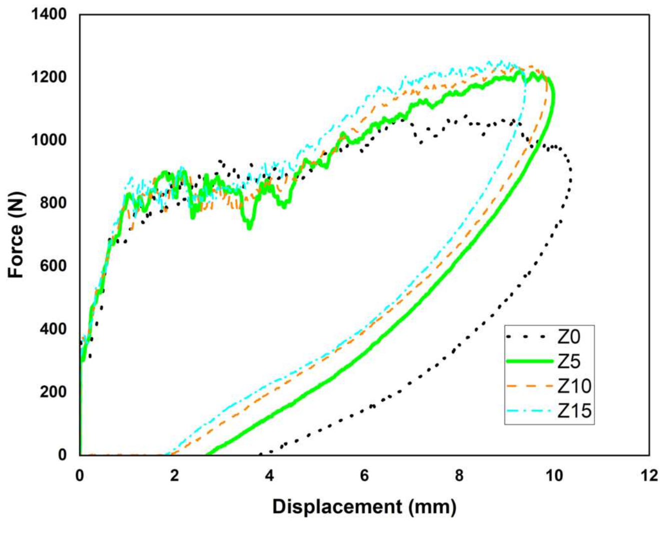


**Figure 5.** Load—displacement plot.

However, in case of Z15, the difference in the magnitude of load between $P_{critical}$ and $P_{threshold}$ was infinitiesimal. This observation indicates that matrix crack propagation inititated at lower loads for the Z15 than the other cases such that premature failure occurred leading to the least energy absorption.

The load—displacement plot from the drop-weight impact test is illustrated in figure 5. The load bearing ability of the composites infused with zirconia fillers at various weight proportions were found to be impreoved as represented by the higher magnitude of peak load. Furthermore, a closed loop pattern was observed for the load—deformation plot in case of the composites with and without fillers tested at an impact energy of 10 J. According to Nunes *et al* [19], the closed loop pattern signifies the absence of perforation in the composite.

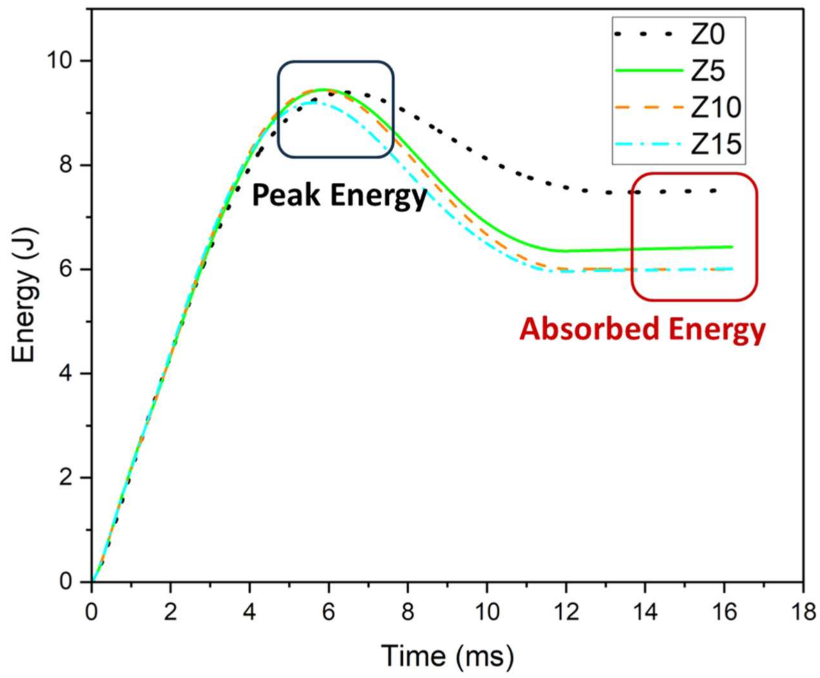


**Figure 6.** Energy—time response.

**Table 4.** Parameters from the drop weight impact test.

| Specimen | Peak force (N) | Peak energy (J) | Energy absorbed (J) | Total deformation (mm) |
|---|---|---|---|---|
| Z0 | 1078.580 | 7.141 | 7.470 | 3.973 |
| Z5 | 1218.838 | 8.610 | 6.351 | 2.791 |
| Z10 | 1236.60 | 9.055 | 6.006 | 2.046 |
| Z15 | 1252.525 | 8.567 | 5.961 | 1.927 |

The influence of $ZrO_2$ proportion in the laminate can be seen from the peak force, peak energy and total energy tabulated in table 4. The composites infused with zirconia fillers were found to have better load bearing ability as observed from the higher magnitude of peak load with respect to the increase in zirconia proportion from 5 wt% to 15 wt%. The peak load increased by 13%, 15% and 16% respectively due to the addition of 5, 10 amd 15 wt% ZrO2 into the matrix respectively. An increasing trend similar to that of the peak force was observed for the peak energy (figure 6). However, the energy absorbed decreased significantly for the composites infused with $ZrO_2$ fillers (table 4). The declining values of absorbed energy for the composites infused with zirconia filler can also be inferred from the decrease in the area under the load-displacement plot and lower displacement values than the composite specimen without filler.

### 3.2. Effect of zirconia on failure behavior and damage area

The morphological images of the impacted specimens are shown in figures 7(a)–(h). The general observation from the images is that failure occurred in the impact zone as localized damage in the form of cracks in the front face (figures 7(a), (c), (e) & (g) and rear face (figures 7(b), (d), (f) & (h)) of the composite respectively. The cracks appeared to propagate away from the impact zone in both the horizontal (lognituidnal) and vertical (transverse) direction. The matrix crack experienced by the laminate in the front face and rear face at low impact energy is a typical failure caused by the localized stress transfer of the impinging impactor onto the laminate and subsequently, the impactor rebounds without causing perforation. The crack growth pattern in the longitudinal and tranverse direction are consistent with the recently reported studies on the drop-weight impact behavior of jute/epoxy composites [20, 21]. Thus, while the degree of damage is relatively less severe at low impact energies, at higher impact energies, the impactor perforates into the composite causing a dent on the front face and cross-shaped bulge on the rear face accompanied by extensive cracking, delamination and fibre breakage [22].

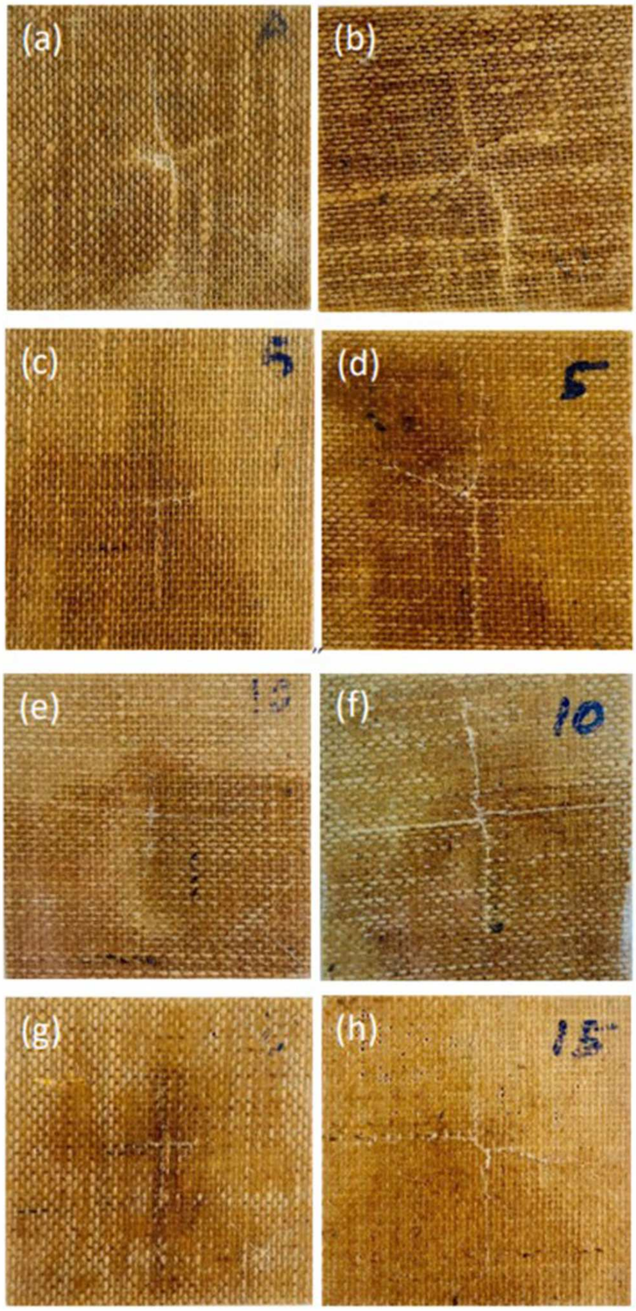


**Figure 7.** Morphological images of composites subjected to impact (a) Front Face—Z0, (b) Rear Face—Z0, (c) Front Face—Z5, (d) Rear Face—Z5, (e) Front Face—Z10, (f) Rear Face—Z10, (g) Front Face—Z15, and (h) Rear Face—Z15.

The images shown in figures 8(a)–(d) provides the crack pattern of the front face of the composites processed from the SketchAndCalc platform. The crack pattern of the rear face of the composites processed from the SketchAndCalc platform is illustrated in figures 9(a)–(d) along with the C-scan images (figure 9(e)–(h)). Following are the major observations from the processed images: (i) Failure occurred by crack propagation in the longitudinal and transverse direction for both the front face and rear face, (ii) In case of the rear face, in addition to the major cracks, multiple number of minor cracks originated and propagated along the transverse direction.

A recent study on the drop-weight impact performance of the jute/polylactic acid composites highlighted that the crack length characteristics and damage area measured from the C-scan images were more accurate than the data obtained from the optical image processing technique [23]. This correlation was also similar in the present study where the processed images of the rear face from the 'SketchAndCalc' platform portrayed only linear crack while the C-scan images depicted the real damage zone around the vicinity of the crack. Thus, in this work, the crack length measurement along the longitudinal and transverse direction and damage area assessment were considered only from the C-scan images. Table 5 depicts

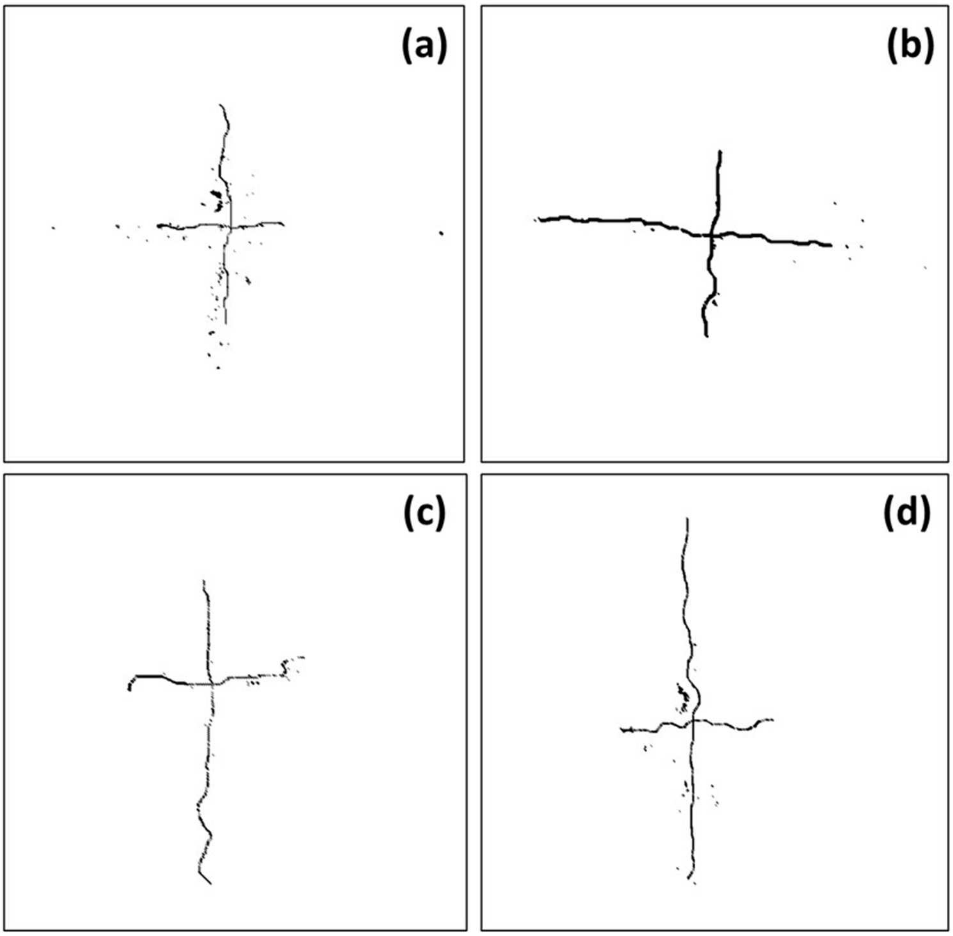


**Figure 8.** Crack pattern in the front face (a) Z0, (b) Z5, (c) Z10 and (d) Z15.

**Table 5.** Crack characteristics from the C-scan images.

| Composite | Major cracks | | Minor cracks along scan axis | Damage area ($mm^2$) |
|---|---|---|---|---|
| | Crack length in the index axis (mm) | Crack length in the scan axis (mm) | | |
| Z0 | 41.65 | 41.83 | No | 49.30 |
| Z5 | 45.29 | 40.05 | Yes | 34.30 |
| Z10 | 40.51 | 44.57 | Yes | 43.36 |
| Z15 | 45.72 | 40.88 | Yes | 57.89 |

the crack lengths and surface damage area computed from the C-scan images. The firsthand observation is the nearly identical or uniform crack length in the longitudinal and transverse direction for the Z0 without filler. As the filler addition is increased, the crack lengths measured along the longitudinal and transverse direction is not uniform or of varying length. The presence of zirconia fillers along the crack path could have played a role in altering its propagation leading to uneven crack formation in the longitudinal and transverse direction. Furthermore, addition of zirconia at 5 wt% and 10 wt% resulted in lower damage area than the Z0 without filler while further addition of $ZrO_2$ filler to 15 wt% leads to increase in damage area. The decrease in damage area with respect to the filler addition at lower filler loadings and the increase in damage area at higher filler loading is consistent with the observations reported in the literature [24, 25].

The surface morphology of the jute/epoxy composites with and without zirconia reinforcement is presented in figures 10(a)–(d). Z0 composite without $ZrO_2$ nanoparticles appears to have a smooth exhibits large voids and interfacial gaps, indicating poor adhesion between the jute fibers and epoxy matrix surface. With the addition of 5 wt% zirconia (figure 10(b)), the surface reveals the presence of dispersed zirconia particles within

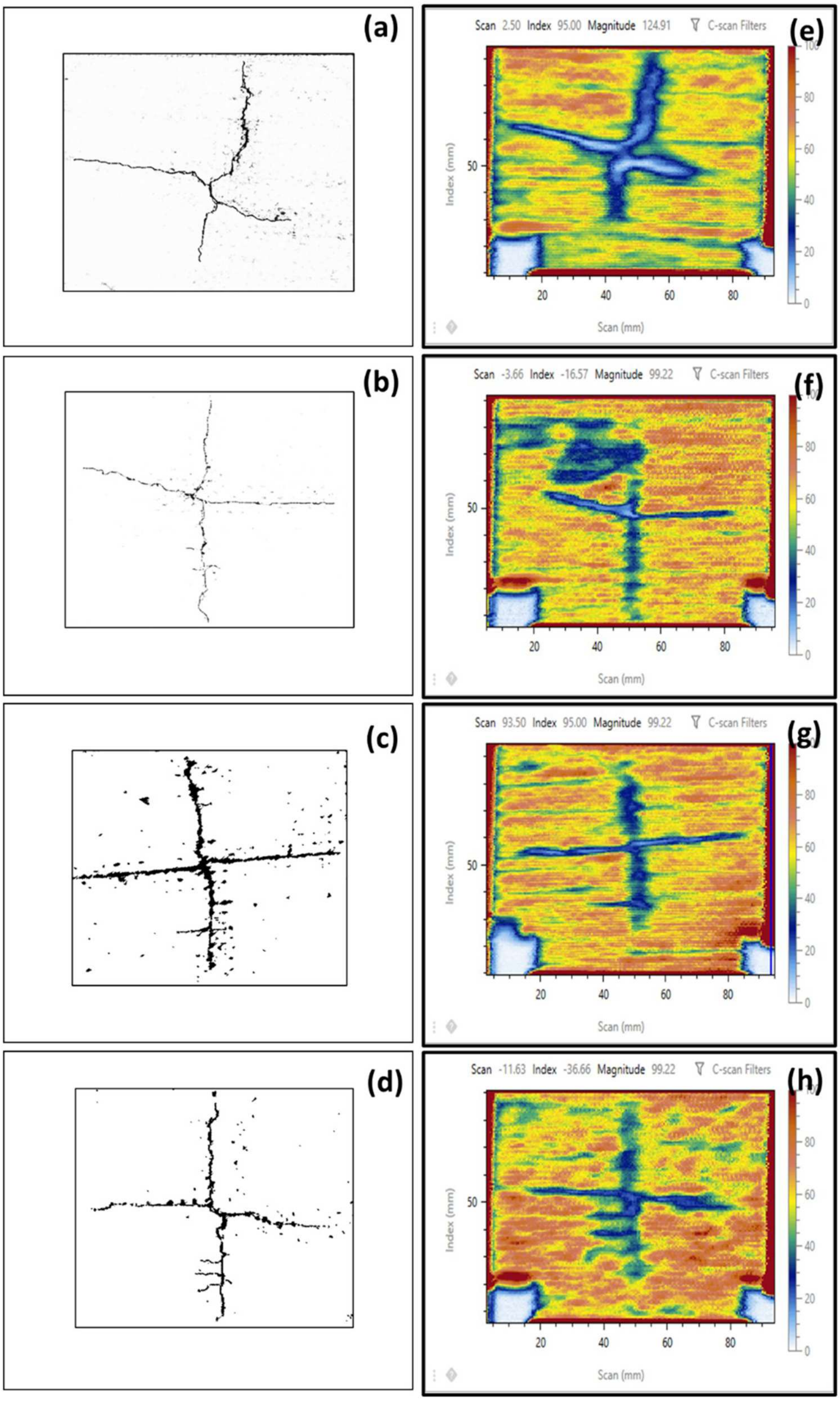


**Figure 9.** Ultrasonic C-scan images of the rear face of the composites (a) Z0, (b) Z5, (c) Z10 and (d) Z15.

the matrix, resulting in reduced porosity and improved particle–matrix interaction. At 10 wt% zirconia loading (figure 10(c)), a more homogeneous distribution of zirconia particles is evident, leading to a denser microstructure. However, when the zirconia content is increased to 15 wt% (figure 10(d)), severe particle agglomeration becomes noticeable, which introduces stress concentration sites and deteriorates the interfacial bonding with the matrix. Such agglomeration negatively affects stress distribution and may promote brittle fracture, thereby diminishing the beneficial effect of zirconia addition.

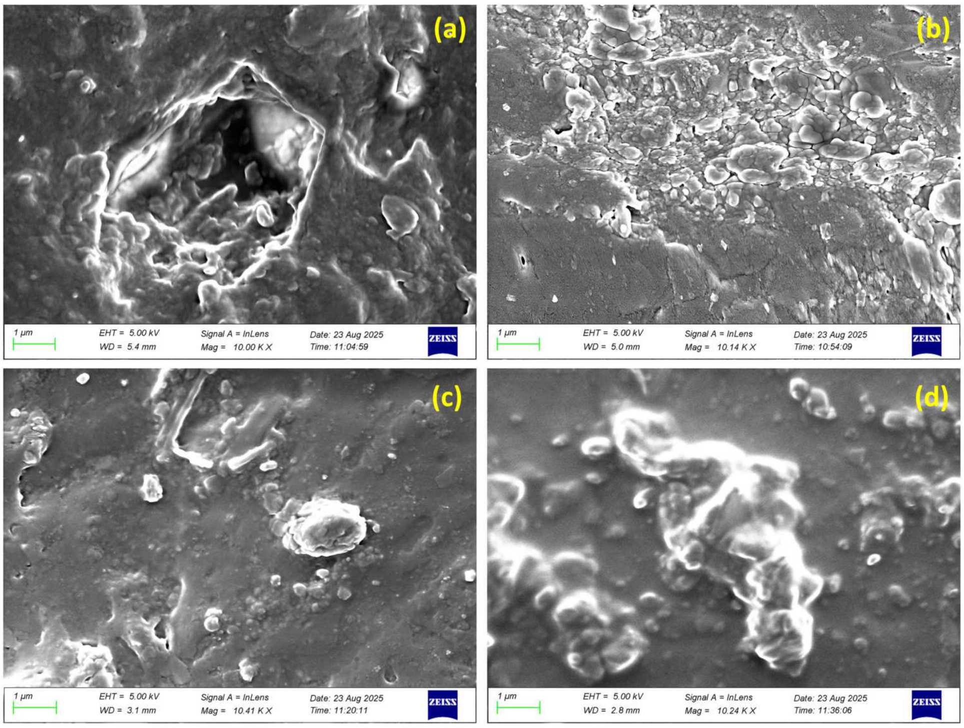


**Figure 10.** Microstructural images from the scanning electron microscope (a) Z0, (b) Z5, (c) Z10 and (d) Z15.

The damage area is correlated to the peak force (figure 11(a)) and absorbed energy for the composites with and without zirconia filler. It is clear from the images that the increase in $ZrO_2$ concentration in the matrix enhances the load bearing ability while the damage area increases. On the contrary, a declining trend was observed with respect to the energy absorbption over the increase in damage area. The major inference from the figures 11(a) and (b) is that the Z5 is the optimum combination where least damage area is observed for a substantial increase in peak force with slight loss in the energy absorption over the other composite configurations with higher proportion of zirconia fillers. The green demarcation line in the plots also indicates Z15 could be the least preferred material due to the significant loss in energy absorption while having greater damage area. The prominent loss in energy absorption characteristics and increase in the damage area at higher filler loading of $ZrO_2$-graphene oxide filler was also observed for the basalt/epoxy composite and the inferior damage tolerance behaviour has been associated with the agglomeration of the $ZrO_2$-graphene filler and their non-uniform dispersion within the matrix [26].

## 4. Conclusion

The damage tolerance behaviour of the jute/epoxy composite filled with zirconium dioxide ($ZrO_2$) filler from 5 wt% to 15 wt% subjected to low velocity impact was examined in this work. Addition of $ZrO_2$ filler enhances the load bearing ability of the jute/epoxy composite with the improvement of approximately 12%—15%. The extent of damage and energy absorbing ability was influenced by the filler loading. Higher filler loading was detrimental to the impact performance as observed from the decline in energy absorption primarily due to nanoparticle agglomeration and the embrittling effect at higher loadings. The observed failure mechanisms were dominated by longitudinal and transverse cracks, with higher filler concentrations promoting the formation of multiple fine transverse cracks. Notably, ultrasonic C-scan analysis provided deeper insight into subsurface delamination and a more realistic representation of the damage footprint compared to optical image-based evaluation. Overall, the jute/epoxy composite with 10 wt% $ZrO_2$ reinforcement exhibited an optimal balance of improved peak load resistance and reduced damage area, making it a promising candidate for applications such as UAV airframes, automotive panels, and protective casings where lightweight design and moderate impact resistance are required.

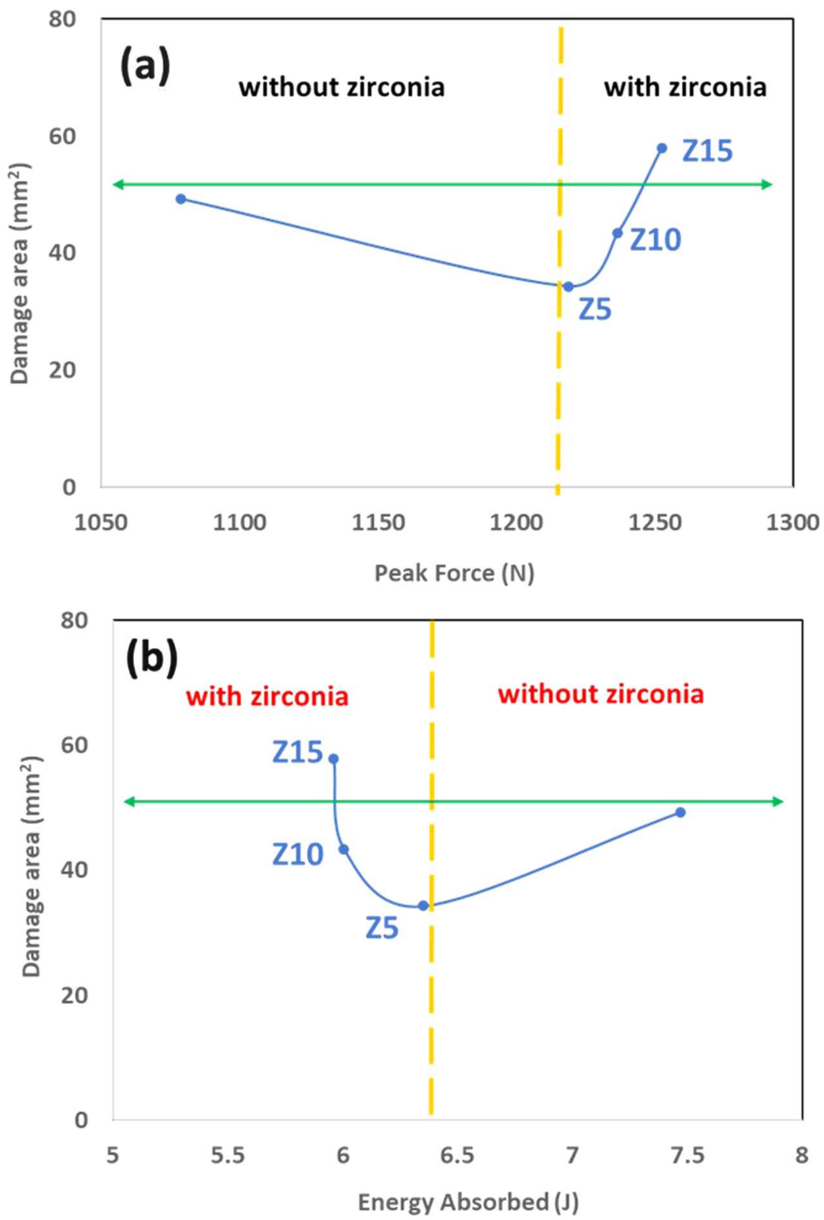


**Figure 11.** Damage area (a) Against Peak force and (b) Against Energy absorbed.

## Data availability statement

No new data were created or analysed in this study. Data will be available from 31 July 2025.

## Author contributions

Dharshini Devi
Conceptualization (equal), Data curation (equal)

Chandrasekar Muthukumar 0000-0002-3637-7630
Senbagan Muthusamy
Conceptualization (equal), Data curation (equal), Resources (equal)

Senthilkumar Krishnasamy 0000-0001-6981-6196
Senthil Muthu Kumar Thiagamani 0000-0003-1443-7222
Conceptualization (equal), Formal analysis (equal), Writing – review & editing (equal)

# References


[1] Siddiqui M A S, Rabbi M S and Dewanjee S 2023 Low-velocity impact response of natural fibre reinforced composites: a comprehensive review on influential parameters *Composites Part C: Open Access* **12** 100422

[2] Mahmud M Z A, Rabbi S M F, Islam M D and Hossain N 2025 Synthesis and applications of natural fiber-reinforced epoxy composites: a comprehensive review *SPE Polymers* **6** 1−19

[3] Purohit A *et al* 2024 A novel study on the stacking sequence and mechanical properties of Jute-Kevlar-Epoxy composites *Interactions* **245** 100

[4] Chandrasekar M, Ishak M R, Jawaid M, Sapuan S M and Leman Z 2018 Low velocity impact properties of natural fiber-reinforced composite materials for aeronautical applications *Sustainable Composites for Aerospace Applications* (Elsevier) 293–313

[5] Kazemi M E *et al* 2021 Investigating the roles of fiber, resin, and stacking sequence on the low-velocity impact response of novel hybrid thermoplastic composites *Compos B Eng* **207** 108554

[6] Alagesan P K 2020 Recent advances of hybrid fiber composites for various applications *Hybrid Fiber Composites* (Wiley) 381–404

[7] Gangil B, Ranakoti L, Verma S, Singh T and Kumar S 2020 Natural and synthetic fibers for hybrid composites *Hybrid Fiber Composites* (Wiley) 1–15

[8] Kamatchi T, Saravanan R, Rangappa S M and Siengchin S 2023 Effect of filler content and size on the mechanical properties of graphene-filled natural fiber-based nanocomposites *Biomass Convers Biorefin* **13** 11311–20

[9] Jagadeesh P, Puttegowda M, Mavinkere Rangappa S and Siengchin S 2021 Influence of nanofillers on biodegradable composites: a comprehensive review *Polym. Compos.* **42** 5691–711

[10] Mishra S K, Purohit A, Palanimuthu S and Kumar A 2025 Exploring the use of TiO2 filler in short ficus benghalensis natural fibre-based polymeric composites *Plast. Rubber Compos.* **54** 69–81

[11] Ahmad I, Bashir M, Sadaqat A, Riaz S and Naseem S 2015 Effects of temperature on zirconia nanoparticles during and after synthesis *Mater. Today Proc.* **2** 5786–92

[12] Devnani G L and Sinha S 2019 Effect of nanofillers on the properties of natural fiber reinforced polymer composites *Mater. Today Proc.* **18** 647–54

[13] Prasob P A and Sasikumar M 2019 Viscoelastic and mechanical behaviour of reduced graphene oxide and zirconium dioxide filled jute/epoxy composites at different temperature conditions *Mater Today Commun* **19** 252–61

[14] Prasob P A and Sasikumar M 2018 Static and dynamic behavior of jute/epoxy composites with ZnO and TiO2 fillers at different temperature conditions *Polym. Test.* **69** 52–62

[15] Lohbauer U *et al* 2010 Zirconia nanoparticles prepared by laser vaporization as fillers for dental adhesives *Acta Biomater.* **6** 4539–46

[16] Mahesh V, Joladarashi S and Kulkarni S M 2018 Suitability study of jute-epoxy composite laminate for low and high velocity impact applications *AIP Conf. Proc.* 1943 (AIP Publishing)

[17] Faruk O, Bledzki A K, Fink H-P and Sain M 2012 Biocomposites reinforced with natural fibers: 2000–2010 *Prog. Polym. Sci.* **37** 1552–96

[18] ASTM D 5628 2007 *Impact Resistance of Flat, Rigid Plastic Specimens by Means of a Falling Dart* (ASTM INTERNATIONAL)

[19] Nunes S G, Reichwald L G G, Júnior W F A, Manes A and Amico S C 2018 Quasi-static indentation and low-velocity impact response of aramid/epoxy composites *4th Brazilian Conferece o Composite Materials* 323–9

[20] Patil S, Mallikarjuna Reddy D, Naveen J, Swamy S S, P V and Venkatachalam G 2022 Low-velocity impact and compression after impact properties of hemp and jute fiber reinforced epoxy composites *J. Nat. Fibers* **19** 12309–24

[21] Islam A *et al* 2024 Response of short jute fibre preform based epoxy composites subjected to low-velocity impact loadings *Composites Part C: Open Access* **14** 100488

[22] Najeeb M I *et al* 2021 Low-velocity impact analysis of pineapple leaf fiber (PALF) hybrid composites *Polymers (Basel)* **13** 3194

[23] Papa I, Lopresto V, Simeoli G, Langella A and Russo P 2017 Ultrasonic damage investigation on woven jute/poly (lactic acid) composites subjected to low velocity impact *Compos B Eng* **115** 282–8

[24] Rahman M *et al* 2013 Effects of amino-functionalized MWCNTs on ballistic impact performance of E-glass/epoxy composites using a spherical projectile *Int. J. Impact Eng.* **57** 108–18

[25] Eslami-Farsani R and Shahrabi-Farahani A 2017 Improvement of high-velocity impact properties of anisogrid stiffened composites by multi-walled carbon nanotubes *Fibers Polym.* **18** 965–70

[26] Toorchi D, Khosravi H and Tohidlou E 2021 Synergistic effect of nano-ZrO2/graphene oxide hybrid system on the high-velocity impact behavior and interlaminar shear strength of basalt fiber/epoxy composite *J. Ind. Text.* **51** 277–96